Southern Oscillation Extremes Reconstructed from Tree Rings of the Sierra Madre Occidental and Southern Great Plains

DAVID W. STAHLE AND MALCOLM K. CLEAVELAND

Department of Geography, University of Arkansas, Fayetteville, Arkansas

(Manuscript received 7 June 1991, in final form 25 November 1991)

ABSTRACT

The El Niño–Southern Oscillation (ENSO) is correlated with climate and tree growth over northern Mexico and the southern Great Plains of the USA. Warm events favor moist-cool conditions from October through March (event years 0 and +1), and subsequent tree growth (year +1) in the region tends to be above average. The opposite climate and tree growth conditions prevail with less consistency during cold events. ENSO-sensitive tree-ring chronologies from this region were selected to develop two reconstructions of the Southern Oscillation index (SOI) back to 1699. For the first reconstruction, a multiple regression-based calibration equation between prewhitened and regionally averaged tree-ring data from Mexico and Oklahoma and a prewhitened winter (DJF) SO index during the period 1900–71 were used to estimate the winter SOI for each year from 1699 to 1971. The tree-ring predictors account for 41% of the winter SOI variance from 1900 to 1971, and the reconstructed SO indices are significantly correlated with independent winter SO indices available from 1866 to 1899.

Because correlation analyses indicate that SO extremes have a much stronger influence on climate and tree growth over Mexico and the southern United States than near-normal SO indices, a second reconstruction of just winter SOI extremes was also developed. Discriminant function analysis based on the growth anomalies at eight individual tree-ring sites located in Mexico, Texas, and Oklahoma was used to classify 56 years from 1699 to 1965 into two opposite winter SOI "extremes" (i.e., $\geqslant 0.5$ or $\leqslant -0.5$). Using a high posterior probability of membership in either extreme category ($P \geqslant 0.65$), and ignoring classifications of near normal winter SO indices, the discriminant functions identified 27 years as winter SOI extremes during the calibration period from 1866 to 1965 (56 extremes actually occurred; reliability = 48%). However, 5 of the 27 classified extremes were actually near-normal indices (post agreement = 81%). With a reasonably stationary relationship between Mexico/Southern Plains climate and winter SOI, validation tests indicate that the reliability of the classification-based reconstruction is about 50%, with a post agreement of at least 70%. These calibration and validation results suggest that the 56 extremes classified from 1699 to 1965 represent about half of the true number of extremes during this 267-year period, and that each reconstructed extreme has up to a 70% chance of representing a true winter SOI extreme.

The most accurate estimates of past winter SOI extremes may be achieved in those years when the regression and classification methods of reconstruction agree, but comparisons with the instrumental data indicate that evidence for a past extreme cannot be disregarded when based on only one method. Both reconstructions indicate an increase in the frequency of winter SOI extremes after ca. 1850. Because the regression and classification errors are randomly distributed through time, these and other reconstructed changes in event frequency may reflect real changes in the extratropical influence of the SO over Mexico and the southern United States, if not in the SO itself.

1. Introduction

The El Niño–Southern Oscillation (ENSO) is the most important cause of interannual variations in the global climate presently known (Rasmusson and Wallace 1983; Folland et al. 1990). Large differences in event magnitude and frequency recorded during the instrumental period have stimulated interest in paleoclimatic evidence for past ENSO variability. The various instrumental indices of the ENSO phenomenon contain quasi-periodic components concentrated at the biennial and 4–5-year frequencies (e.g., Trenberth 1976; Rasmusson et al. 1990), but the timing, magnitude, and worldwide climatological impacts of recurrent ENSO extremes vary substantially. The record 1982–83 El Niño event was associated with catastrophic drought and wildfire in Australasia and with torrential rainstorms and coastal flooding in the western Americas, while fewer weather and climate anomalies developed worldwide during the 1957–58 and 1972–73 El Niño events (e.g., Glantz et al. 1987). ENSO indices also suggest possible decade-scale changes in the frequency of warm and cold extremes (e.g., Enfield 1989; Trenberth and Shea 1987). Warm and cold events seem to have decreased in frequency and intensity during the 1930s and 1940s, and warm events have

Corresponding author address: Dr. David W. Stahle, University of Arkansas, Department of Geography, 108A Ozark Hall, Fayetteville, AR 72701.

dominated the period from 1977 to 1988 (e.g., Wolter and Hastenrath 1989; Trenberth 1990). Unfortunately, the available meteorological records of ENSO are not long enough to determine how typical or long lasting this important decade-scale ENSO variability may be. Archival and proxy climate records have been used to extend the record of past ENSO activity (e.g., Quinn et al. 1978, 1987; Lough and Fritts 1985, 1990; Michaelsen 1989) and may provide the long-term data needed to investigate the apparent decadal variability of the ENSO phenomenon. In this paper, we report a strong and regionally coherent ENSO signal in tree-ring chronologies from northern Mexico and the United States southern Great Plains and use the most ENSO-sensitive chronologies to reconstruct and analyze an index of the Southern Oscillation (SO) from 1699 to 1971.

The search for an ENSO signal in old-growth trees near the Gulf of Mexico should be productive because a strong cool-season (October–March) teleconnection has been detected between the ENSO and temperature and precipitation data from the Gulf region (e.g., Douglas and Englehart 1981; Ropelewski and Halpert 1986, 1987, 1989; Kiladis and Diaz 1989; Cavazos and Hastenrath 1990). Contrary to many regions worldwide, winters in the southern USA and northern Mexico tend to be cool and wet during warm events or El Niño episodes and warm and dry during cold events (Ropelewski and Halpert 1986, 1989). This cool-season teleconnection to the Gulf of Mexico region is remarkably consistent, and during warm events may reflect a dynamical link between enhanced convection in the eastern tropical Pacific, an enhanced Hadley circulation, and an accelerated subtropical jet stream over Central America and the Gulf of Mexico (Bjerknes 1969). An ENSO influence on tree growth in this region can be expected because the ENSO teleconnection to regional temperature and precipitation extends into the early spring growing season and because low-elevation trees in the Gulf of Mexico region often break dormancy as early as February during warm winters (e.g., Stahle 1990). There may also be a preconditioning effect on spring–summer tree growth from cool-season ENSO events due to soil moisture depletion during cold events or soil moisture recharge during warm events.

In spite of these favorable circumstances, there are also limitations to the strength of any ENSO signal in these tree-ring data. First, the ENSO phenomenon falls well short of explaining all climate variance over the Gulf of Mexico region, and even the most carefully selected trees from the most climate sensitive forest sites are not perfect sensors of the prevailing climate. Therefore, the clean ENSO signal from the tropical Pacific is inevitably degraded to some extent by its registration in tree-ring proxies of the extratropical climate. Second, the ENSO teleconnection is usually not strong during the late spring and summer season, which are important to tree growth in the southern United States. Finally, the ENSO influence in northeast Mexico may reverse sign and favor summer climate anomalies that contrast with the winter teleconnection (Cavazos and Hastenrath 1990). These considerations are necessary for a proper evaluation of the ENSO signal in Mexican and Southern Plains tree-ring chronologies, which we demonstrate are muted but not hopelessly biased recorders of the extratopical influence of ENSO extremes during the cool season over the Gulf of Mexico region.

2. Previous tree-ring studies of ENSO

Several recent studies have reported an ENSO influence on tree-ring data (e.g., Stahle 1990; Swetnam and Betancourt 1990; D'Arrigo and Jacoby 1991; Cleaveland et al. 1992; Meko 1992), and three tree-ring reconstructions of past ENSO variations have been published (Lough and Fritts 1985, 1990; Michaelsen 1989). Most of these studies have been based on North American tree-ring data, but the strongest and most consistent ENSO signal in these particular data appears to be found in northern Mexico and the southern United States. This tree growth response to ENSO-forced climate anomalies is consistent with the nature of the ENSO influence detected in meteorological data from Mexico and the southern United States and will be substantiated by our analyses of additional tree-ring data from the region.

Studies of the ENSO signal in tree-ring chronologies from the Southern Hemisphere have been limited and generally less successful (Lough and Fritts 1985, 1990), but substantial progress is still needed in the development of a geographic network of Southern Hemisphere chronologies and in understanding the climatic response of these chronologies. Tropical forests have proven largely intractable for dendrochronology (Jacoby 1989), but the amount of research in the tropics has been totally inadequate considering the number of available tree species. Jacoby and D'Arrigo (1990) have reported interesting analyses of teak (*Tectona grandis*) from Java. Teak may become an especially valuable ENSO proxy because Java is under the western center of action of the Southern Oscillation.

3. The data

The tree-ring chronologies used in this study were collected from the southern United States by the University of Arkansas Tree-Ring Laboratory (e.g., Stahle et al. 1985) and from northern Mexico by M. A. Stokes, T. H. Naylor, T. P. Harlan, and others at the University of Arizona Laboratory of Tree-Ring Research. All of the southern United States series studied were collected during or after 1980 and are based primarily on deciduous oaks (especially post oak, *Quercus stellata*) and bald cypress (*Taxodium distichum*). The Mexican chronologies were collected between 1960 and 1974 from mountain sites above 1800 m, and the dataset analyzed included 11 Douglas fir (*Pseudotsuga menziesii*), 3 ponderosa pine (*Pinus ponderosa*), 3 Jeffrey pine (*P. jeffreyi*), and 1 white fir (*Abies concolor*) chronologies.

The tree-ring chronologies were based on increment cores from over 20 trees per site and were exactly dated by dendrochronologists at the Universities of Arizona and Arkansas. The Mexican chronologies represent the mean value of all standardized ring width measurement series available for each year, and were developed with the computer programs INDEX and SUMAC (Graybill 1979). The southern United States chronologies were also based on an average of standardized measurements using the program ARSTAN (Cook 1985; Cook and Holmes 1985). Standardization is necessary to remove long-term growth trend and differences in absolute growth rate (Fritts 1976). All of these tree-ring chronologies have varying degrees of low-order growth persistence believed to be largely biological in origin (e.g., Cook 1985). Because the tree growth persistence cannot be readily discriminated from climatic persistence, autoregressive (AR) modeling (Box and Jenkins 1976) was used to remove serial correlation from both the tree-ring chronologies and the winter SO indices prior to calibration. The AR-modeled persistence structure observed in the winter SO indices was subsequently added to the tree-ring estimates of winter SOI following calibration with regression (see below). Prewhitening tree-ring chronologies prior to their use in regression analyses with prewhitened climate data and then adding the persistence structure of the instrumental climate data to the reconstruction (e.g., Meko 1981) is a reasonable alternative to the development of regression models that use lagged tree-ring variables (i.e., prior growth values) to account for possible climate influences on persistence in the tree-ring data.

An SO index extending from 1866 to 1984 was used as a measure of the ENSO phenomena (Ropelewski and Jones 1987; Jones 1988; and obtained from P. D. Jones, personal communication). This index is based on the sea level pressure difference between Tahiti and Darwin after the annual pressure cycle was removed from both series and the resulting monthly anomaly series were normalized by the monthly standard deviations (Ropelewski and Jones 1987). Missing data for Tahiti and Darwin in the early portion of the index were estimated with available pressure data from surrounding stations, often far removed from either Tahiti or Darwin (Jones 1988).

4. ENSO signal in tree-ring data near the Gulf of Mexico

Differences in the seasonality of the ENSO signal in tree-ring data from the Gulf region were first identified with correlation analyses. The post oak chronologies from the Southern Plains are most highly correlated with a boreal winter and spring average (December–May) of the SOI, with correlations varying up to −0.45 ($P < 0.001$). However, the Mexican tree-ring chronologies from higher elevation forests in the Sierra Madre are most strongly correlated with a fall and winter average (Oct–Feb) of the SOI, which may reflect in part an ENSO influence on winter precipitation (Cavazos and Hastenrath 1990) and its subsequent effect on tree growth in spring through the soil moisture reservoir. Based on these results, the winter SOI (DJF) was selected to measure the ENSO and its common influence on tree growth in both the southern United States and northern Mexico. The winter SOI is a good compromise because ENSO events often reach maturity and the associated extratropical influences are often strongest during this season (e.g., Rasmusson and Carpenter 1982). However, it may also be possible to reconstruct a longer seasonal average of the SOI with tree-ring data from Mexico and Texas.

Significant negative correlations between winter SOI and tree growth were found in a large region extending from southern Oklahoma across northern Mexico for the period 1900–71 (Fig. 1). The highest correlations were observed for trees growing along the crest of the Sierra Madre Occidental. This inverse correlation with the SOI is consistent with the nature of the ENSO teleconnection to the Gulf of Mexico region documented with meteorological data (e.g., Douglas and Englehart 1981; Ropelewski and Halpert 1986, 1989; Kiladis and Diaz 1989). Warm event years and negative SO indices tend to be associated with cool and wet conditions during the cool season, while cold event years and positive SO indices are often linked with a warm and dry fall–winter–spring climate over northern Mexico and the

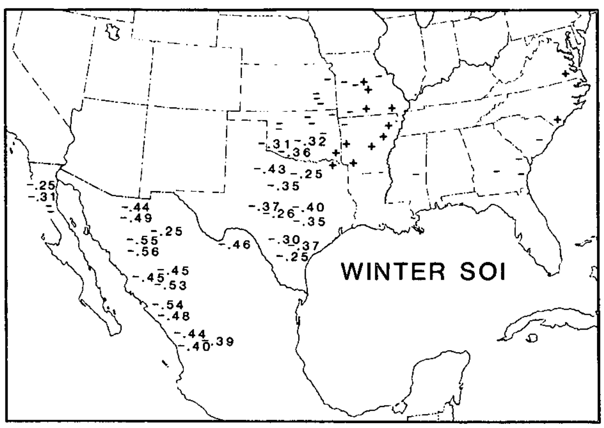

FIG. 1. Correlation coefficients computed between the winter SOI and selected moisture-sensitive tree-ring chronologies for the period 1900 to 1971 (the chronologies were not prewhitened, and four of the Mexican chronologies ended in 1965). Significant correlations ($P \leq 0.05$) are indicated by the coefficients, nonsignificant correlations are indicated by sign only.

southeastern United States. Consequently, wide tree rings tend to form in this region during the spring and summer following a warm event, and narrow growth rings tend to form after a cold episode.

The tree-ring and SOI correlations suggest that the ENSO influence on tree growth and climate tends to fade from Mexico northward into the Great Plains (Fig. 1), which is roughly consistent with the geographic pattern of the ENSO signal in precipitation data reported by Douglas and Englehart (1981). The strongest warm events, however, appear to be associated with increased cloudiness and rainfall during spring and with increased tree growth in Arkansas and Missouri (Stahle et al. 1991).

5. Calibration and verification based on a regression model

Correlation and stepwise multiple regression analyses between the prewhitened winter SOI and the network of prewhitened tree-ring chronologies in Mexico and the southern United States were used to identify those chronologies with the strongest SOI signal. The two or three most SOI-sensitive tree-ring chronologies in each of Mexico, Texas, and Oklahoma were then used to compute three regional tree-ring averages [i.e., chronologies from Creel, Chihuahua (Douglas fir) and Nuestra Senora de Guadalupe, Durango (ponderosa pine); Brazos River, Mason Mountain, and Nichols Ranch, Texas; and Lake Arbuckle and Lake Keystone, Oklahoma (all post oak, Stahle et al. 1985)]. These three regional averages were then entered into a stepwise multiple regression analysis as candidate predictors of the winter SOI for the period 1900–71. The regional chronologies for Mexico and Oklahoma were selected as predictors of winter SOI on the basis of a significant F ratio ($P \leqslant 0.05$) and variance explained. Although the tree-ring average for Texas is significantly correlated with the SOI, it was not selected in the stepwise regression because it is also strongly correlated with the Mexican tree-ring average and contributes little additional information about the SO.

The multiple regression model using the Mexican and Oklahoma chronologies was the best of several evaluated and explained 41% of the variance in the prewhitened winter SOI during the calibration period from 1900 to 1971 after downward adjustment for loss of degrees of freedom (adjusted $r^2 = 0.41$, $P \leqslant 0.001$). Past winter SO indices were estimated with the following calibration equation:

$$\hat{Y}_i = 3.29 - 2.07X_{1i} - 1.14X_{2i}, \qquad (1)$$

where $\hat{Y}_i$ is the prewhitened estimate of the winter SOI in year i, and X_{1i} and X_{2i} are the prewhitened tree-ring indices in year i for the Mexican and Oklahoma chronology averages, respectively. Autoregressive (AR) modeling was used to prewhiten the full winter SOI time series available for 1866 to 1988. An AR(2) model was selected, with coefficients of −0.03 and −0.26, respectively. These coefficients were added to the tree-ring estimates of winter SOI from A.D. 1699 to 1971 to complete the reconstruction. This modification is small, but nevertheless assumes that the persistence structure of the winter SOI observed since 1866 is representative of the past ±300 years. The AR(2) model is consistent with the persistence structure of the Tahiti–Darwin SOI identified by Trenberth (1984) for the period 1935–82, but its validity prior to 1866 still remains to be independently tested.

The negative coefficients and the larger fraction of variance associated with the Mexican chronology [Eq. (1)] are physically consistent with the nature of the ENSO teleconnection in this region. Warm events (negative SO indices) favor cool-wet conditions and good tree growth, and this influence appears to be strongest in northern Mexico (e.g., Douglas and Englehart 1981; Fig. 1). The Oklahoma chronology only contributes an additional 7% to the SOI variance explained by this model, but this contribution is statistically significant and presumably reflects an expansion of teleconnected climate effects into the Southern Plains during many ENSO extremes. The regression residuals are normally distributed and homoscedastic and are not autocorrelated (based on the Durbin–Watson test statistic), suggesting that the calibration model is free of any large systematic bias. This apparent randomness of the regression error is crucial to the interpretation of changes in the frequency of reconstructed SOI extremes discussed below.

Independent winter SO indices available from 1866 to 1899 were used to evaluate the accuracy of the calibration equation. Although these early SO are probably less reliable than the 20th century data, they nevertheless represent one of the few direct instrumental measurements of the SO during the late 19th century and are useful for the validation of the tree ring–SOI regression model.

The strong agreement between the observed and reconstructed series during the calibration interval (1900–71) is only slightly reduced during the verification period (1866 to 1899, Fig. 2), and some of the differences can be attributed to the lower quality SO indices available before 1990. The reconstructed SO indices are significantly correlated with the actual indices from 1866 to 1899 ($r = +0.51$, $P < 0.0001$), and a two-tailed t-test on the difference between the observed and reconstructed means during the same time period is not significant. A sign test indicates that actual and estimated departures from the mean have the same sign in over 90% of the years ($P \leqslant 0.01$, Conover 1980), and cross-products t tests indicate that observed and reconstructed departures of opposite sign are usually small (i.e., close to the mean, $P \leqslant 0.01$). The reduction of error statistic (Fritts 1976) is +0.24, indicating that the reconstruction is providing more unique information about the winter SOI than might theoretically

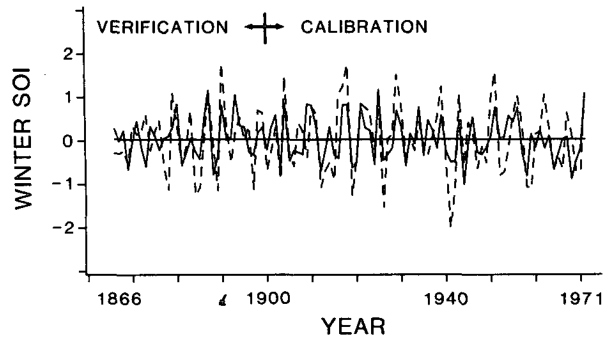

FIG. 2. Observed (dashed line) and reconstructed (solid line) winter SOI from 1866 to 1971. The reconstruction was calibrated using multiple regression analysis between two regionally averaged tree-ring chronologies and the winter SOI from 1900 to 1971 [Eq. (1)] and is well correlated with independent SO indices during the verification period (1866–1899).

be derived from an estimate based solely on the mean SOI during the calibration period (1900–71).

Because the tree-ring data calibrate only 41% of the variance in the winter SOI, it is clear that factors other than the SO are responsible for a large fraction of the climate and tree growth variance in the Gulf of Mexico region. Nevertheless, the calibration and verification statistics do indicate that unique and potentially useful information about past fluctuations in the winter SOI may be present in the reconstruction, particularly if these reconstructions are considered with other archival or proxy estimates of past ENSO activity.

The data illustrated in Fig. 2 also suggest that the tree-ring reconstruction might in fact be a more faithful proxy of large magnitude winter SO events than suggested by the overall variance explained. Close examination of Fig. 2 reveals that many of the strongest agreements between reconstructed and actual winter SO indices occurred during relatively large positive and negative SO departures (e.g., 1887, 1903, 1904, 1912, 1921, 1925, 1956, 1958, and 1971), and many of the largest disagreements occurred when the actual SOI was near normal (e.g., 1907, 1908, 1914, 1935, 1954, and 1968). The greater influence of SO extremes is certainly logical because little extratropical response would be expected when the SO is near normal. The larger influence of SO extremes on climate and tree growth in the Gulf of Mexico region can be demonstrated with correlation analyses restricted to extreme (winter SOI $\leqslant -0.5$ and $\geqslant 0.5$) and uneventful years (winter SOI > -0.5 and < 0.5) from 1866 to 1971. For example, the correlation between state-averaged June PDSI from Texas and winter SOI extremes is -0.49 ($P \leqslant 0.001$) but falls to -0.13 during the uneventful years [June PDSI from 1888–1982 was used because it is very highly correlated with Texas tree growth (Stahle and Cleaveland 1988)]. Similar changes in the winter SOI signal were detected in selected tree-ring chronologies from Mexico and the Southern Plains. Michaelsen (1989) and others have also noted the logical importance of the strongest ENSO events on North American tree-ring data.

6. Calibration and verification based on discriminant function analysis

Discriminant function analysis of low, near-normal, and high SO indices was used to exploit the episodic and spatially variable nature of the ENSO teleconnection to climate and tree growth in Mexico and the Southern Plains and to supplement the regression-based estimates of past winter SOI extremes. In this application, discriminant function analysis can only provide a categorical classification of past SO indices, but it may be more effective at exploiting spatial variability in the ENSO signal than our simple regression model, which used just two regional averages as predictors.

The unwhitened winter SO indices from 1866 to 1965 were first arbitrarily separated into three categories (1965 is the ending year for one of the Mexican chronologies). These three categories are SOI $\leqslant -0.5$ (referred to as warm events), SOI > -0.5 and < 0.5 (near-normal years), and SOI $\geqslant 0.5$ (cold events), which represent 28%, 44%, and 28% of the years from 1866 to 1965, respectively. Three linear classification functions based on the spatial patterns of tree growth at eight SOI-sensitive tree-ring sites located across northern Mexico, Texas, and Oklahoma were then used to classify each year into one of the three winter SOI categories (Appendix). The eight chronologies were not prewhitened and were selected from the network of available chronologies with stepwise discriminant function analysis (SAS Institute 1985). This selection includes two Douglas fir (El Salto-west, Durango; Sierra del Carmen, Coahuila), one ponderosa pine (Nuestra Senora de Guadalupe, Durango), and five post oak chronologies (Lavaca River, Yegua Creek, and Nichols Ranch in Texas; and Mud Creek and Lake Arbuckle in Oklahoma) (Stahle et al. 1985).

The classification functions correctly classified 64% of all years from 1866 to 1965 into their appropriate winter SOI category based simply on the highest posterior probability for membership in one of the three groups. The results of this initial three-category classification are summarized with a contingency table and associated verification scores in the Appendix (see Table A2). Because the initial analysis included a number of incorrect classifications, we choose to maximize classification accuracy by raising the posterior probability threshold for group membership to $P \geqslant 0.65$ (Figs. 3, 4, and 5; Appendix) and by omitting all classifications of near-normal winter SO indices (little climate impact over Mexico or the Southern Plains would be expected when the SO is near normal). These additional classification constraints increased the accu-

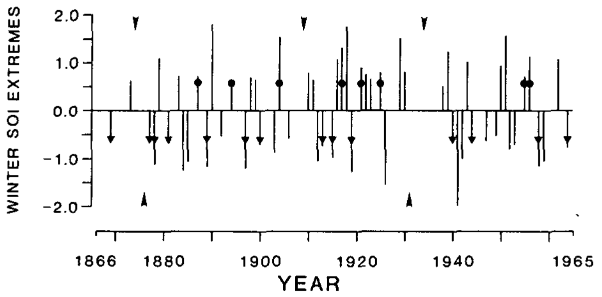

FIG. 3. Vertical lines indicate the actual values of 56 winter SOI "extremes" that exceed the ±0.5 thresholds from 1866 to 1965. Circles denote positive extremes (⩾0.5) and triangles indicate negative extremes (⩽ −0.5) that were correctly classified by the discriminant function analysis (Appendix). Arrows indicate five estimated extremes actually associated with near normal SO indices.

racy of the discriminant function-based reconstructions (i.e., improved the post agreement score; Appendix), but only at the expense of identifying a smaller fraction of all winter SOI extremes that actually occurred in the past (i.e., the prefigurance and reliability scores; Appendix). Nevertheless, this trade-off is warranted and largely unavoidable because all winter SO extremes do not influence the Mexico–Southern Plains climate, and SO extremes are not the sole cause of climate and tree growth anomalies in this region.

Using the more stringent criteria for group membership, the discriminant function correctly classified 39% of all winter SOI extremes that actually occurred from 1866 to 1965 (i.e., prefigurance = 39%, 22 of 56, Fig. 3; Appendix). However, five additional near normal years were misclassified as extremes (i.e., false alarms; Appendix). In order to properly interpret the classification-based *reconstruction* of extremes, it is important to estimate the probability that any given classified extreme in the preinstrumental period is accurate (i.e., post agreement; Appendix). Using the more stringent threshold for group membership ($P \geqslant 0.65$), winter SOI extremes are classified 48% as often as the actual frequency from 1866 to 1965 (i.e., reliability = 27 of 56; Appendix and Fig. 3), including the five misclassified extremes that were actually near-normal years. During the calibration period the discriminant function classifies some 48% of the total number of winter SOI extremes with a hit rate near 81% (i.e., post agreement = 81%, 22 of 27) and with very little chance that a classified extreme actually belongs to the opposite category (i.e., 0 of 27).

The classification of positive and negative winter SOI "extremes" was asymmetrical, however, and a larger fraction of negative (warm) extremes were classified with greater accuracy. Classified negative winter SOI extremes recorded from 1866 to 1965 had a reliability of 57% (16 of 28) with 87% post agreement (i.e., 2 of the 16 ⩽ −0.5 SOI classifications were actually near normal, Fig. 3). However, classified positive SOI extremes recorded from 1866 to 1965 had a reliability of only 39% (11 of 28) with 73% post agreement (i.e., 3 of the 11 ⩾ 0.5 SOI classifications were actually near normal, Fig. 3). These classification results suggest that negative winter SOI extremes may be one of the major causes of wet/favorable tree growth conditions during the winter and spring over northern Mexico and the Southern Plains, whereas positive winter SOI extremes may be only one of several causes of dry/poor tree growth conditions during the winter–spring in this region. Asymmetry is not evident, however, in the analyses of rainfall data for the Gulf of Mexico region by Ropelewski and Halpert (1986, 1989), although their analyses were based on different definitions of warm and cold events, their rainfall data covered a shorter time period, and they did not investigate tree-ring data. Also, some of the apparent asymmetry might only reflect differences in the degree to which positive and negative winter SOI extremes beyond the ±0.5 thresholds actually represent well-developed cold and warm ENSO events and their associated worldwide teleconnection patterns (e.g., Barnston et al. 1991). However, comparisons between years with winter SOI "extremes" and the warm and cold ENSO event years identified by Ropelewski and Halpert (1986) and by Kiladis and Diaz (1989) from 1877 to 1965 do not indicate any major differences between the two categories of winter SOI extremes (i.e., both categories include and omit nearly the same number of warm or cold ENSO events, and both extreme categories include almost the same number of years not listed as well-developed warm or cold events).

A subperiod analysis for the 100-year period from 1866 to 1965 was used to validate the classifications of past SOI extremes comparing the tree-ring classifications with independent SO indices. Five separate discriminant functions were computed for five 80-year

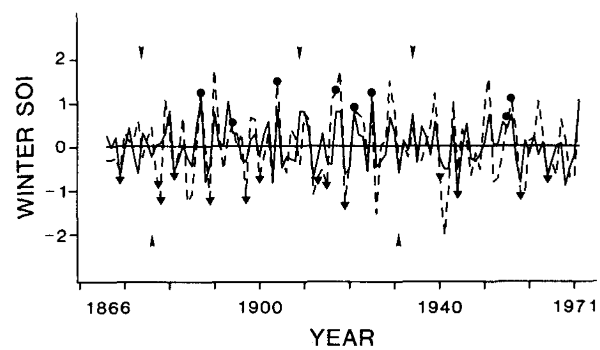

FIG. 4. A comparison between the regression (solid line) and classification-based reconstructions (symbols as defined in Fig. 3) and the actual winter SO indices (dashed line) available from 1866 to 1971 (the classifications end in 1965, the last year available for one Mexican chronology). Note the agreement with the instrumental SO indices when both the regression and classification methods estimate winter SO indices beyond the ±0.5 thresholds.

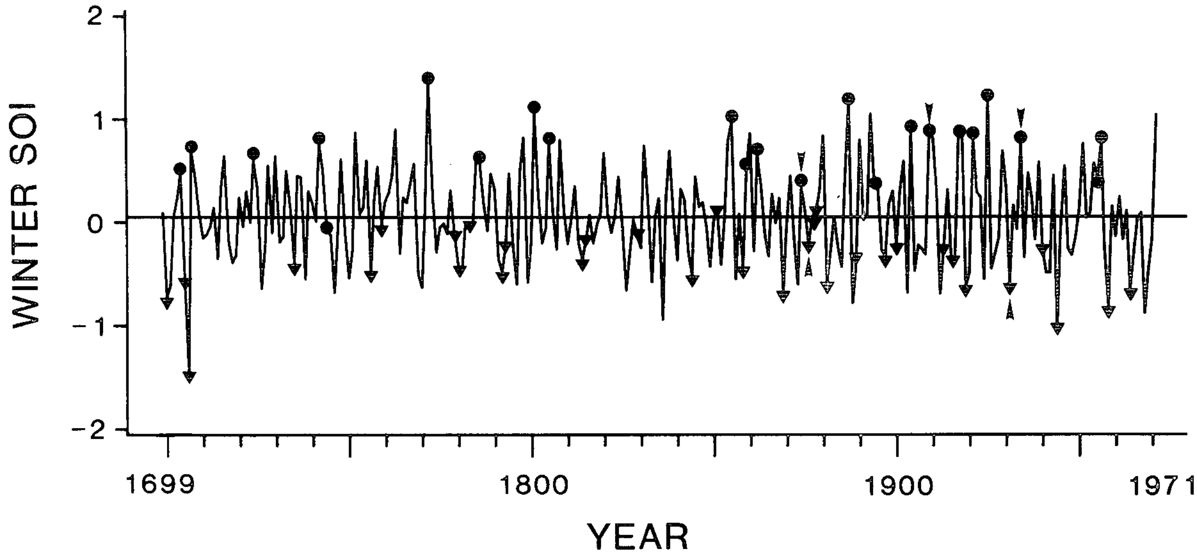

FIG. 5. Reconstructed winter SOI from 1699 to 1971. The solid line is the regression-based reconstruction, the symbols (defined in Fig. 3) represent years classified by the discriminant function as positive and negative winter SOI extremes. Note the asymmetry in the classified positive (23) and negative extremes (33) and the increased frequency of classified and regression-estimated SOI extremes after 1850.

subperiods between 1866 and 1965 (which differed only by the specific 20-year period excluded), and the tree-ring classified extremes (based on posterior probabilities $\geqslant 0.65$) were then compared with the actual SOI data available for the remaining nonoverlapping 20-year subperiods. Although each of these discriminant functions was based on only 80 years of data, the overall classification reliability for independent SOI extremes was 50% (28 of 56), actually slightly better than the full period calibration. This included seven false classifications of what were actually near-normal indices and one outright misclassified opposite extreme for a post agreement of 71% (20 of 28). With a reasonably stationary relationship between Mexico–Southern Plains climate and winter SOI, these verification tests suggest that the use of discriminant function analysis to identify SOI extremes in the Mexican and Southern Plains tree-ring data should enable one to identify about one-half of the total *number* of all past SOI extremes with up to a 70% hit rate. The validation prefigurance is 36% (20 of 56), only a small decrease from the calibration prefigurance of 39%.

The discriminant-based reconstruction using the full period (1866–1965) and a posterior probability of $\geqslant 0.65$ missed the two most extreme negative (i.e., 1926, 1941) and the two most extreme positive winter SO indices (i.e., 1890, 1918) actually observed between 1866 and 1965 (Fig. 3). The posterior probabilities for these four years, however, all exceeded 50% for their appropriate category. In fact, the threshold at which the posterior probability for group membership is set involves some compromise between the correct classification of extreme events and the number of false classifications. False classifications have been minimized in this particular analysis, but for some applications such as cross-validation between different proxies of the ENSO it may be important to maximize the percentage of correct classifications.

The more accurate classification of negative rather than positive winter SOI extremes is a major difference between the discriminant and regression-based reconstructions. Regional drought is often more spatially coherent than regional wet years, and the discriminant analysis based on the eight tree-ring chronologies seems to take advantage of spatially complex moisture anomalies during years with negative winter SOI extremes more effectively than our simple regression model based on just two regionally averaged tree-ring predictors. The multiple regression model also tends to force symmetry in the derived reconstruction because the sum of squared departures from the regression line fit to the data is minimized. This might explain the differences in symmetry between the two reconstructions. However, the actual influence of positive and negative winter SOI extremes on tree growth and possibly climate anomalies over Mexico and the Southern Plains might also be somewhat asymmetrical, in spite of evidence to the contrary in the precipitation analyses of Ropelewski and Halpert (1986, 1989). Tree growth integrates precipitation and temperature in a manner not unlike the soil moisture model embodied in the Palmer drought severity index. Tree growth is highly correlated with the June PDSI in Texas ($r = 0.77$, Stahle and Cleaveland 1988), and there is some evidence for asymmetry in the winter SOI influence on the Texas state-averaged June PDSI compiled by Karl et al. (1983). The correlation between the winter SOI and Texas June PDSI decreases from −0.30 (P = 0.13) during the 27 years from 1888 to 1982 when winter SOI was ≤ −0.5 to +0.14 during the 28 years when it was ≥ +0.5. Also, 81% of the negative winter SOI extremes (≤ −0.5) between 1888 and 1982 were followed by above-average Palmer drought indices for June in Texas (i.e., wet conditions in 13 of 16 years), but only 67% of the positive winter SOI extremes were followed in Texas by below-average June drought indices (i.e., dry conditions in 14 of 21 years). The average June PDSI for the 16 warm events was +2.43 (moderate wetness) and −1.28 (mild drought) for the 21 cold events.

7. Comparison of the regression and discriminant function-based reconstructions

Given the differences between the regression and classification-based reconstructions, the most accurate estimate of past winter SOI extremes might be achieved when the two methods agree on the categorical identification of an extreme (Table 1). The two methods of reconstruction are compared with the actual winter SO indices from 1866 to 1971, and an SOI extreme (≥0.5 or ≤ −0.5) was never identified that was opposite from the extreme actually measured (Fig. 4). Also, the two reconstructions usually agree on the categorical identification of extremes from 1866 to 1965 (Fig. 4), and even though the two methods share three predictor chronologies, it is still reassuring to note that they never estimate opposite winter SOI extremes for any given year from 1699 to 1965 (see the reconstruction below).

In spite of the many agreements between the two methods of reconstruction, there are interesting differences. The classification approach is less detailed and is only categorical, but it can succeed in the accurate identification of winter SOI extremes when the regression approach fails (e.g., 1877, 1878, 1915). However, two of the five near-normal SO indices misclassified as extremes by the discriminant analysis were well approximated by the regression estimates (i.e., 1876 and 1934, Fig. 4). Although greater confidence in a reconstructed extreme might be justified when the two methods agree (see below), these examples indicate that a reconstructed SOI extreme cannot be disregarded if estimated by only one method.

TABLE 1. Winter SOI extremes reconstructed by both the regression and classification methods (observed winter SOI shown in parentheses after 1866).

Winter SOI ≤ −0.5	Winter SOI ≥ 0.5
1700	1707
1705	1724
1706	1742
1756	1772
1792	1789
1844	1801
1869 (−0.55)	1805
1881 (−0.57)	1855
1919 (−1.26)	1862
1931 (−0.43)	1887 (1.16)
1944 (−0.57)	1904 (1.47)
1958 (−1.07)	1909 (−0.38)
1964 (−0.68)	1917 (1.24)
	1921 (0.85)
	1925 (0.72)
	1934 (0.42)
	1956 (1.03)

The differences between the reconstructions can partly be explained by differences in the predictor chronologies and methods of computation used, but the classification analysis also indicates that there can be important spatial structure to the regional ENSO signal that may not be most effectively exploited by the multiple regression analysis using the regionally averaged chronologies. For example, contrasting spatial patterns of tree growth developed during the negative index year of 1877, and the discriminant function correctly classified an SOI extreme totally missed by the regression model (Fig. 4). A strong El Niño event developed during the winter of 1876–77 (Ropelewski and Halpert 1987; Kiladis and Diaz 1989; Fig. 4), and tree growth was well above average in the southern Sierra Madre and in most of east Texas and eastern Oklahoma but was below average elsewhere in the region. As a result, one of the two tree-ring chronologies included in both the Mexican and Oklahoma regional averages used to estimate winter SOI was below average. Below-average growth is normally associated with high SO indices (cold events), and the regression estimate during 1877 was for a near-zero SOI (−0.01, Fig. 4). The classification function, however, used the discontinuous pattern of well-above-average tree growth to correctly classify a negative SO extreme in 1877 (i.e., ≤ −0.5). These results indicate that the regression and classification methods for reconstruction both have advantages and limitations, but a careful review of Fig. 4 suggests that the most accurate categorical reconstruction of SOI extremes may be achieved when both methods estimate winter SOI ≥ 0.5 or ≤ −0.5 (Table 1). There are 15 years from 1866 to 1965 when the regression and classification methods estimate extremes beyond the ±0.5 threshold, and 12 of these years were correct (Table 1). This is the same level of accuracy achieved with the classification results alone (~80%), but two of the three misses were very close to being correct (i.e., +0.42 and −0.43 for reconstructed positive and negative extremes, respectively), and the reconstruction of extremes based on the concurrence of both methods is symmetrical. To interpret these results optimistically, when the two methods of reconstruction agree on the categorical identification of an extreme, there may be over a 90% chance that the winter SOI average was close to, if not beyond, the ±0.5 threshold.

8. Reconstructed winter SOI: 1699–1971

The regression- and classification-based reconstructions of winter SOI from 1699 to 1971 are presented together in Fig. 5 (the classifications end in 1965), and the winter SOI extremes reconstructed by both methods are listed in Table 1. These reconstructions suggest long-term changes in the frequency and intensity of winter SO extremes since 1699. The most striking changes are the early 19th century decrease and the late 19th–early 20th century increase in winter SO extremes. This is suggested by the changing variance of the regression-based estimate and by the large increase in the number of classified SOI extremes after 1850 (the average interval between classified extremes of either sign was 6.04 years before 1850 and only 3.71 years after; Fig. 5). Previous tree-ring investigations of ENSO, based for the most part on different tree-ring chronologies, have noted comparable changes in reconstructed amplitude (Lough and Fritts 1985; Michaelsen 1989).

There are many caveats that complicate the interpretation of an SOI reconstruction accounting for only 41% of the observed SOI variance and that are based on proxies of an extratropical climate, which itself is influenced partly by ENSO and partly by other factors. The reconstructed changes in event frequency in the late 19th century, however, are certainly plausible because similar decade-scale changes in the frequency and intensity of ENSO events are evident in the meteorological record (e.g., Rasmusson and Wallace 1983; Trenberth and Shea 1987), including strong oscillations from about 1880 to 1920 (e.g., Trenberth 1990). Model studies indicate that long period changes in ENSO activity are possible given changes in sea surface temperatures (SST) in the tropical Pacific (Graham 1990), and decade-scale shifts in SST data from the Pacific have been matched by long-term changes in the SO (Wolter and Hastenrath 1989). Furthermore, the reconstructed changes in event frequency (Fig. 5) may in fact reflect real changes in the extratropical influence of the winter SO, if not in the SO itself, because the residual errors associated with the multiple regression used to reconstruct the winter SOI are normally distributed and random through time. If this random error component were added to the reconstructed time series, the large 19th and 20th century changes in reconstructed SOI variance should remain.

Spectral and cross-spectral analyses indicate that 27% of the reconstructed winter SOI variance is concentrated at periods from 3.7 to 4.0 years, and the reconstruction is strongly coherent ($P \leqslant 0.01$) with the observed SO indices at these frequencies (Cleaveland et al. 1992). We designed a bandpass filter and applied it to the instrumental and 272-year reconstruction of winter SOI in order to emphasize this 4-year frequency component (Cleaveland et al. 1992). This filtered version of the reconstructed winter SOI is not shown, but it indicates several sharp changes in the amplitude of this particular frequency component, including a large amplitude increase in the early 20th century that is apparent in both the reconstructed and observed winter SO indices (Cleaveland et al. 1992).

Many of the El Niño events identified in the historical record by Quinn et al. (1978, 1987) and Hamilton and Garcia (1984) are matched by negative SOI estimates in the reconstruction, and several other estimates preceded or followed the historical events by ±1 year. However, several historical events are not evident in the reconstructions, and several strongly negative reconstructed SO indices also classified as extremes by the discriminant function (Table 1) are not registered in the archival record. There are several possible reasons for these discrepancies, including: 1) the ENSO influence on wet and dry years with above- and below-average tree growth in northern Mexico and the Southern Plains is not unique (e.g., Lough and Fritts 1990), and the other causes of climate variability are not adequately differentiated by this particular reconstruction; 2) the tree-ring chronologies are not perfect proxies of regional climate; 3) the available archival record of past El Niño activity is fragmentary and the past El Niño events identified in these archives did not necessarily excite large-scale climate anomalies in the extratropics (Quinn et al. 1987); and 4) the climate of northern Mexico and the Southern Plains does not always respond in precisely the same fashion to even very strong El Niño events. These considerations imply that the Mexican and Southern Plains tree-ring data might be more faithful proxies of the actual extratropical influence of the SO in the Gulf of Mexico region than may be suggested by the fraction of variance explained for a reconstruction of the SOI based on Tahiti–Darwin pressure data. This argument cannot be logically invoked when using tree-ring data to estimate the immediate regional climate (e.g., regional precipitation and temperature), but may have some merit when considering the growth influences of climate forcing from remote regions such as the tropical Pacific.

If the changes in the frequency and intensity of reconstructed SO indices can be more accurately interpreted as changes in the extratropical forcing of climate over the Gulf of Mexico region by the SO, then low-frequency variations in the winter SOI reconstruction (Fig. 5) have important implications for seasonal forecasts over the southern United States and Mexico, which are based in part on conditions in the tropical Pacific.

9. Conclusions

The results summarized in Figs. 1 and 4 indicate that the available tree-ring chronologies from Mexico and the Southern Plains register one of the strongest and most spatially coherent ENSO signals yet detected in proxy climate data worldwide. The ENSO signal in these tree-ring data may be exceeded only by the ENSO evidence in historical archives (e.g., Quinn et al. 1987), in the physical and chemical properties of annually layered corals in the Pacific (e.g., Shen et al. 1987), and possibly in tree-ring data from teak forests of Java (e.g., Jacoby and D'Arrigo 1992). Because of the practical difficulties involved in the development of a well-replicated regional array of centuries-long coral chronologies, archival records and the tree-ring chronologies from Mexico and the southern United States may remain for some time as the most accessible high-quality proxies of past ENSO activity.

In spite of the valuable insight into the ENSO phenomenon that these tree-ring chronologies can provide, the network of available chronologies from Mexico and the southern United States has many deficiencies. The spatial and temporal coverage of these chronologies are both incomplete, and many old-growth forest remnants remain to be sampled. For example, none of the isolated high-elevation conifer forests of the Sierra Madre Oriental in Nuevo Leon, southern Coahuila, or Tamaulipas have ever been evaluated for dendroclimatology. Also, the existing Mexican chronologies (largely confined to the Sierra Madre Occidental) were collected between 1960 and 1974. Consequently, any calibration of these chronologies with indices of ENSO will have spatial limitations and will omit comparisons with the largest warm event (i.e., 1982–83) and two of the largest cold events in the instrumental record (i.e., 1973, 1975). Many of the ENSO sensitive chronologies from the Southern Plains were collected before 1983, and few extend earlier than 1700 (Stahle et al. 1985). Unfortunately, the prospects for rectifying these deficiencies are fading in portions of northern Mexico and the southern United States where logging and deforestation continue to destroy remnant old-growth forests. Historic buildings in Mexico and the United States may preserve old timbers suitable for chronology extension back to perhaps 1500 or 1600, but many of these unique structures are also disappearing.

Even if the network of climate sensitive tree-ring chronologies can be improved in Mexico and the southern United States, these data alone will not be sufficient to achieve the ultimate goal of developing the most accurate and detailed possible reconstruction of the ENSO phenomenon for the past several centuries. However, the reasonably consistent and recurrent pattern of global climate anomalies teleconnected with the warm and cold extremes of ENSO (Ropelewski and Halpert 1987, 1989) offers a realistic opportunity to develop a very accurate paleoclimatic record of ENSO. As more annually resolved and climate-sensitive proxies become available from the various climate regions influenced by ENSO, it should be possible to use the worldwide teleconnection fingerprint of ENSO extremes encoded in long proxy time series for the accurate, multivariate reconstruction of past ENSO variability.

Acknowledgments. This research was supported by the National Science Foundation, Climate Dynamics Program (Grant ATM-8914561), and the NOAA Climate and Global Change Program (Grant NA 98AA-D-AC199). We thank D. M. Meko for providing data from Mexico; M. A. Stokes, T. P. Harlan, and T. H. Naylor for developing the Mexican chronologies; P. D. Jones and K. R. Briffa for the Southern Oscillation Index used in this study; R. S. Cerveny for suggesting the application of discriminant analysis; R. E. Livezey and two anonymous reviewers for editorial suggestions; and G. G. Hawks for assisting in the development of the Southern Plains tree-ring data. We especially thank Dr. James E. Dunn for extensive statistical advice and assistance.

APPENDIX

Winter SOI Reconstructions Based on Discriminant Function Analysis

Linear classification functions were applied to three categories of winter SOI (warm event $\leqslant -0.5$; near normal > -0.5 and <0.5; cold event $\geqslant 0.5$). The prior probabilities for group membership observed in the instrumental winter SO indices from 1866 to 1965 were 0.28, 0.44, and 0.28 for the warm, normal, and cold categories, and these probabilities were included in the computation of the constant. The following equation was used to compute the probability that the growth values observed at the eight tree-ring sites in a given year belonged to one of the three SOI categories:

$$P_i = \frac{e^{S_i(\mathbf{y})}}{e^{S_1(\mathbf{y})} + e^{S_2(\mathbf{y})} + e^{S_3(\mathbf{y})}}, \qquad \text{(A1)}$$

where

P_i the posterior probability computed for each category of winter SOI ($_i$ = 1, 2, 3 or warm, normal, cold) for each year,

e 2.71828+

S_i score from the classification function (a summation of the constant and weighted tree-ring indices) for each category of winter SOI(i),

$\mathbf{y}$ vector of tree-ring indices for each year.

TABLE A1. The constants and chronology weights used in the three versions of the classification function to compute the posterior probability of membership in each of the three SOI categories.

	Warm event	Normal	Cold event
Constant	−41.84	−31.74	−27.34
El Salto	30.06	25.59	28.28
Guadalupe	11.84	8.71	5.40
Carmen	4.67	2.71	1.66
Lavaca	5.52	4.77	4.04
Yegua	2.55	4.53	4.35
Nichols	4.48	2.79	1.73
Arbuckle	28.43	25.89	22.49
Mud	−15.08	−11.61	−9.87

TABLE A2. Contingency table and selected scores computed for the tree-ring classifications of years from 1866 to 1965 into three categories of winter SOI, based only on the highest posterior probability of membership in a category.

	Tree-ring classifications of winter SOI by category			
Actual winter SOI by category	Warm (SOI ≤ −0.5)	Normal (SOI < 0.5, > −0.5)	Cold (SOI ≥ 0.5)	Total
SOI ≤ −0.5	19	7	2	28
percent	67.9	25.0	7.1	100.0
SOI < 0.5, > −0.5	6	30	8	44
percent	13.6	68.2	18.2	100.0
SOI ≥ 0.5	2	11	15	28
percent	7.1	39.3	53.6	100.0
Total	27	48	25	100
percent	27.0	48.0	25.0	100.0
Percent correct				64.0%
Post agreement	.70	.63	.60	
False alarm ratio	.30	.37	.40	
Prefigurance	.68	.68	.54	
Reliability	.96	1.09	.89	

The two most heavily weighted chronologies in the classifications for each category of winter SOI (Table A1) are located at the southern and northernmost boundaries of the study area (El Salto and Arbuckle, respectively), implying a connection between regionwide growth anomalies and SO extremes. This represents a slightly different spatial component than that reflected in the regression-based reconstruction because the El Salto chronology was not included in the Mexican chronology average used in Eq. (1). The Carmen, Lavaca, Yegua, and Nichols chronologies are near the center of the study area and have similar weights. The negative sign of the Mud Creek, Oklahoma, weight is questionable because the Arbuckle chronology located 90 km to the east is positively weighted. If real, this difference implies an east–west gradient in Oklahoma moisture anomalies linked to SO extremes.

The results of the initial classification based on Eq. (A1) and the weights listed in Table A.1 are summarized in Table A2. These classifications are based simply on the highest posterior probability for membership in one of the three categories of winter SOI. The scores computed below the contingency table (Table A2) are defined and discussed by Murphy and Daan (1985) and Stanski et al. (1989). The percent correct represents the fraction of all years from 1866 to 1965 classified into the correct winter SOI category. Post agreement is the number of years correctly classified divided by the total classifications for each category and is ideally 100%. The false alarm ratio is 100 minus post agreement and is ideally 0. Prefigurance (or "hit rate"), the most stringent test, is the number of years correctly classified divided by the number of years actually observed in each SOI category and would ideally be 100%. The classification frequency or reliability is the total number of years classified (regardless of accuracy) divided by the total years observed in each category. Reliability values above 100% indicate classification at greater than the observed frequency (overforecasting); values below 100% indicate classification below the observed frequency (underforecasting).

After the initial classification summarized in Table A2, only those years assigned as either warm or cold events based on $P \geq 0.65$ were used to reconstruct past winter SOI extremes. All remaining classifications were ignored, including years classified as near normal based on $P \geq 0.65$. This procedure assumes that winter SOI extremes have a larger extratropical climate influence than years with a near-normal winter SOI. This more stringent classification of SOI extremes also maximizes the overall correct classification of extremes (i.e., post agreement = 81%) and insures that no extremes are mistakenly classified in the opposite category. These improved scores came only at the expense of detecting all past winter SOI extremes (i.e., prefigurance = 39% and reliability = 48%). Nevertheless, because winter SOI extremes (and especially years with near-normal winter SO indices) are not the exclusive cause of climate and tree growth anomalies over Mexico and the Southern Plains, a winter SOI reconstruction that maximizes accuracy is certainly to be preferred.

The classification and regression-based reconstructions of winter SOI, the posterior probabilities computed from the tree-ring data for three categories of winter SOI from 1699 to 1965, and the observed winter SO indices computed from data supplied by P. D. Jones (e.g., Jones 1988) are all available from the authors upon request.

REFERENCES

Barnston, A. G., R. E. Livezey, and M. S. Halpert, 1991: Modulation of Southern Oscillation–Northern Hemisphere midwinter climate relationships by the QBO. *J. Climate*, **4**, 203–217.

Bjerknes, J., 1969: Atmospheric teleconnections from the equatorial Pacific. *Mon. Wea. Rev.*, **97**, 163–172.

Box, G. E. P., and G. M. Jenkins, 1986: *Time Series Analysis: Forecasting and Control.* Holden-Day, 575 pp.

Cavazos, T., and S. Hastenrath, 1990: Convection and rainfall over Mexico and their modulation by the Southern Oscillation. *Int. J. Climatology,* **10**, 377–386.

Cleaveland, M. K., E. R. Cook, and D. W. Stahle, 1992: Secular variability of the Southern Oscillation detected in tree-ring data from Mexico and the southern United States. *El Niño: The Historical and Paleoclimatic Record of the Southern Oscillation,* H. Diaz and V. Markgraf, Eds., Cambridge University Press, 271–291.

Conover, W. J., 1980: *Practical Nonparametric Statistics.* J. Wiley, 493 pp.

Cook, E. R., 1985: A time series approach to tree-ring standardization. Ph.D. dissertation, University of Arizona, 165 pp.

——, and R. L. Holmes, 1985: Users manual for program ARSTAN. Lamont-Doherty Geological Observatory, Columbia University, 29 pp.

D'Arrigo, R. D., and G. C. Jacoby, 1991: A 1000-year record of winter precipitation from northwestern New Mexico, USA: A reconstruction from tree-rings and its relation to El Niño and the Southern Oscillation. *Holocene,* **1**, 95–101.

Douglas, A. V., and P. J. Englehart, 1981: On a statistical relationship between autumn rainfall in the central equatorial Pacific and subsequent winter precipitation in Florida. *Mon. Wea. Rev.*, **109**, 2377–2382.

Enfield, D. B., 1989: El Niño, past and present. *Rev. Geophysics,* **27**, 159–187.

Folland, C. K., T. Karl, and K. Ya. Vinnikov, 1990: Observed climate variations and change. *Clim. Change, The IPCC Scientific Assessment,* J. T. Houghton, G. J. Jenkins, and J. J. Ephraums, Eds., Cambridge University Press, 194–238.

Fritts, H. C., 1976: *Tree-Rings and Climate.* Academic Press, 567 pp.

Glantz, M., R. Katz, and M. Krenz, Eds., 1987: *Climate Crisis.* U.N. Environment Program and NCAR, 105 pp.

Graham, N. E., 1990: Model ENSO cycles under late pleistocene conditions. *Workshop on Paleoclimatic Aspects of El Niño/Southern Oscillation,* Boulder, CO, NOAA and INSTAAR.

Graybill, D. A., 1979: Revised computer programs for tree-ring research. *Tree-Ring Bull.*, **39**, 77–82.

Hamilton, K., and R. R. Garcia, 1986: El Niño/Southern Oscillation events and their associated midlatitude teleconnections 1531–1841. *Bull. Amer. Meteor. Soc.*, **67**, 1354–1361.

Jacoby, G. C., 1989: Overview of tree-ring analysis in tropical regions. *IAWA Bull.*, **10**, 99–108.

——, and R. D. D'Arrigo, 1990: Teak (Tectona grandis L.F.), a tropical species of large-scale dendroclimatic potential. *Dendrochronolgia,* **8**, 83–98.

Jones, P. D., 1988: The influence of ENSO on global temperatures. *Clim. Monitor,* **17**, 80–89.

Karl, T. R., L. K. Metcalf, M. L. Nicodemus, and R. G. Quayle, 1983: Statewide average climatic history, Texas 1888–1982. *Historical Climatology Series,* 6-1, National Climatic Data Center, 39 pp.

Kiladis, G. N., and H. F. Diaz, 1989: Global climatic anomalies associated with extremes in the Southern Oscillation. *J. Climate,* **2**, 1069–1090.

Lough, J. M., and H. C. Fritts, 1985: The Southern Oscillation and tree rings: 1600–1961. *J. Climate Appl. Meteor.*, **24**, 952–966.

——, and ——, 1990: Historical aspects of El Niño/Southern Oscillation—Information from tree-rings. *Global Ecological Consequences of the 1982–83 El Niño–Southern Oscillation,* P. W. Glynn, Ed., Elsevier Oceanography Series, 285–321.

Meko, D. M., 1981: Applications of the Box–Jenkins methods of time series analysis to the reconstruction of drought from tree-rings. Ph.D. dissertation, University of Arizona, 149 pp.

——, 1992: Spectral properties of tree-ring in the United States Southwest as related to ENSO. *El Niño: The Historical and Paleoclimatic Record of the Southern Oscillation,* H. F. Diaz and V. Markgraf, Eds., Cambridge University Press.

Michaelsen, J., 1989: Long-period fluctuations in El Niño amplitude and frequency reconstructed from tree-rings. *Geophys. Monograph,* **55**, 69–74, Amer. Geophys. Union.

Murphy, A. H., and H. Daan, 1985: Forecast evaluation. *Probability, Statistics, and Decision Making in the Atmospheric Sciences,* A. H. Murphy and R. W. Katz, Eds., Westview Press, 379–437.

Quinn, W. H., D. O. Zopf, K. S. Short, and R. T. W. Kuo Yang, 1978: Historical trends and statistics of the Southern Oscillation, El Niño, and Indonesian droughts. *Fish. Bull.*, **76**, 663–678.

——, V. T. Neal, and S. E. Antunez De Mayolo, 1987: El Niño occurrences over the past four and a half centuries. *J. Geophys. Res.*, **92**, 14 449–14 461.

Rasmusson, E. M., and T. H. Carpenter, 1982: Variations in tropical sea surface temperature and surface wind fields associated with the Southern Oscillation/El Niño. *Mon. Wea. Rev.*, **110**, 354–384.

——, and J. M. Wallace, 1983: Meteorological aspects of El Niño/Southern Oscillation. *Science,* **222**, 1195–1202.

——, X. Wang, and C. F. Ropelewski, 1990: The biennial component of ENSO variability. *J. Marine Sys.*, **1**, 71–96.

Ropelewski, C. F., and M. S. Halpert, 1986: North American precipitation and temperature patterns associated with the El Niño/Southern Oscillation (ENSO). *Mon. Wea. Rev.*, **114**, 2352–2362.

——, and ——, 1987: Global and regional scale precipitation patterns associated with the El Niño/Southern Oscillation. *Mon. Wea. Rev.*, **115**, 1606–1626.

——, and P. D. Jones, 1987: An extension of the Tahiti–Darwin Southern Oscillation index. *Mon. Wea. Rev.*, **115**, 2161–2165.

——, and M. S. Halpert, 1989: Precipitation patterns associated with the high index phase of the Southern Oscillation. *J. Climate,* **1**, 268–284.

SAS Institute, Inc., 1985: *SAS User's Guide: Statistics,* Version 5 ed., SAS Institute, Inc., 956 pp.

Shen, G. T., E. A. Boyle, and D. W. Lea, 1987: Cadmium in corals: Chronicles of historical upwelling and industrial fallout. *Nature,* **328**, 794–796.

Stahle, D. W., 1990: The tree-ring record of false spring in the south-central USA. Ph.D. dissertation, Arizona State University, Tempe, 272 pp.

——, and M. K. Cleaveland, 1988: Texas drought history reconstructed and analyzed from 1698 to 1980. *J. Climate,* **1**, 59–74.

——, J. G. Hehr, G. G. Hawks, M. K. Cleaveland, and J. R. Baldwin, 1985: *Tree-Ring Chronologies for the Southcentral United States,* Tree-Ring Laboratory and Office of the State Climatologist, University of Arkansas, Fayetteville, 135 pp.

——, M. K. Cleaveland, and R. S. Cerveny, 1991: Tree-ring reconstructed sunshine duration over central USA. *Int. J. Climatol.*, **11**, 285–295.

Stanski, H. R., L. J. Wilson, and W. R. Burrows, 1989: Survey of common verification methods in meteorology. Environment Canada, Atmospheric Environment Service, Res. Rep. No. (MSRB) 89-5, Downsview, Ontario, 114 pp.

Swetnam, T. W., and J. L. Betancourt, 1990: Fire-Southern Oscillation relations in the southwestern United States. *Science,* **249**, 1017–1020.

Trenberth, K. W., 1976: Spatial and temporal variations of the Southern Oscillation. *Quart. J. Roy. Meteor. Soc.*, **102**, 639–653.

——, 1984: Signal versus noise in the Southern Oscillation. *Mon. Wea. Rev.*, **112**, 326–332.

——, 1990: Recent observed interdecadal climate changes in the Northern Hemisphere. *Bull. Amer. Meteor. Soc.*, **71**, 988–993.

——, and D. J. Shea, 1987: On the evolution of the Southern Oscillation. *Mon. Wea. Rev.*, **115**, 3078–3096.

Wolter, K., and S. Hastenrath, 1989: Annual cycle and long-term trends of circulation and climate variability over the tropical oceans. *J. Climate,* **2**, 1329–1351.